International Journal of Advanced Research in Engineering and Technology (IJARET)
Volume 6, Issue 3, March, 2015, pp. 70-81, Article ID: IJARET_06_03_008
Available online at
http://www.iaeme.com/IJARET/issues.asp?JTypeIJARET&VType=6&IType=3
ISSN Print: 0976-6480 and ISSN Online: 0976-6499

MODELLING ANALYSIS & DESIGN OF DSP BASED NOVEL SPEED SENSORLESS VECTOR CONTROLLER FOR INDUCTION MOTOR DRIVE

A. O. Amalkar
Research Scholar, Electronics & Telecomm. Deptt
S.S.G.M. College of Engineering Shegaon, India

Prof. K. B. Khanchandani
Professor, Electronics & Telecomm. Deptt
S.S.G.M. College of Engineering Shegaon, India

ABSTRACT

Unscented Kalman Filter (UKF), which is an updated version of EKF, is proposed as a state estimator for speed sensorless field oriented control of induction motors. UKF state update computations, different from EKF, are derivative free and they do not involve costly calculation of Jacobian matrices. Moreover, variance of each state is not assumed Gaussian, therefore a more realistic approach is provided by UKF. In order to examine the rotor speed (state V) estimation performance of UKF experimentally under varying speed conditions, a trapezoidal speed reference command is embedded into the DSP code. EKF rotor speed estimation successfully tracks the trapezoidal path. It has been observed that the estimated states are quite close to the measured ones. The magnitude of the rotor flux justifies that the estimated dq components of the rotor flux are estimated accurately. A number of simulations were carried out to verify the performance of the speed estimation with UKF. These simulated results are confirmed with the experimental results. While obtaining the experimental results, the real time stator voltages and currents are processed in Matlab with the associated EKF and UKF programs.

Key words: Unscented Kalman Filter, State Predictions, Covariances, and Digital Signal Processor

Cite this Article: Amalkar, A. O. and Prof. Khanchandani, K. B. Modelling Analysis & Design of DSP Based Novel Speed Sensorless Vector Controller for Induction Motor Drive *International Journal of Advanced Research in*

Engineering and Technology, **6**(3), 2015, pp. 70-81.
http://www.iaeme.com/IJARET/issues.asp?JType=IJARET&VType=6&IType=3

1. INTRODUCTION

Closed-loop drives have superior dynamic performance, and allow for the implementation of energy-saving techniques. Most closed-loop drives require feedback of variables that are either unavailable or expensive to measure. Reliability of the drive is also an important factor when considering feedback: sensors add to the possible points of failure; therefore there has been significant research on "sensorless" control. In reality, it is impossible to achieve a completely "sensorless" closed-loop drive, i.e. having no voltage, current, or speed information. Engineers try to avoid the cost and failures of speed encoders, which initiated research for several speed-sensorless control schemes. Another important variable in vector control is the machine magnetic flux, but its measurement is complex [4]. When closed-loop torque-control is desired, knowledge of the machine electromechanical torque is required, but torque sensors are expensive. Therefore flux, speed, and torque estimators or observers are used to replace expensive and less-reliable sensors. Estimators in motor drives can be categorized into three main groups: back electro-motive force (EMF) methods, model reference adaptive systems (MRAS), and observer-based approaches such as Kalman filters, Luenberger observers, sliding-mode observers, and nonlinear observers. Such estimators differ in terms of estimation errors, dependence on motor parameters, and settling time [5].

The block diagram of a typical induction motor drive is shown in Figure 1 an induction machine is fed by a three-phase inverter from a dc bus [1]. To achieve the desired torque-speed response, the control and estimation algorithms use information from sensors. The speed ω_r, is usually available from a speed encoder. Even though flux measurement can be available from Hall Effect sensors in some applications, flux is usually estimated for cost and reliability reasons, and is not shown in Figure 1. Current (i_{abc}) and voltage (v_{abc}) measurements are usually available, and are used in the flux estimation process. The mechanical load on the machine shaft could be a fan, propeller, vehicle gearbox, etc. This paper presents a high-level procedure for implementing novel estimators on a digital signal processor (DSP) in induction machine applications.

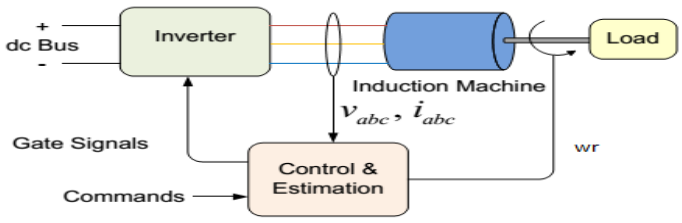

Figure 1 Typical induction motor drive

2. UNSCENTED KALMAN FILTER

EKF is a simple solution derived by direct linearization of the state equation for extending the famous (linear) Kalman filter into nonlinear filtering area. Although it

is straightforward and simple, EKF has well-known drawbacks [2, 6, 7]. These drawbacks include:

- Instability due to linearization and erroneous parameters.
- Costly calculation of Jacobian matrices.
- Biasedness of its estimates.
- Lack of analytical methods for suitable selection of model covariances

UKF is proposed in order to overcome the first three of these disadvantages. The main advantage of UKF is that it does not need linearization in the computation of the state predictions and covariances. Due to this, its covariance and Kalman gain estimates are more accurate [3]. This accurate gain, at the end, leads to better state estimates. In this study, UKF is introduced into the problem of speed and flux estimation of an induction motor. General simulation results are given and a brief comparison is made between speed estimation performances of UKF and EKF. The filtering problem involved in this work is to find the best (in the sense of minimum mean square error (MMSE)) linear estimate of the state vector x_k of the induction machine which evolves according to the discrete-time nonlinear state transition equation.

$$x_{k+1} = f(x_k , u_k) + w_k \tag{1}$$

where f (.,.) is the induction machine dynamics, x k is the state of the induction machine at sampling instant k, u_k is the known input to the induction machine at time k and w_k is the additive white process noise term representing modeling errors. Also, it is assumed that we have a set of noisy measurements z_k which are related to the state vector of the induction machine by the linear relationship;

$$y_k = C\, x_k + v_k \tag{2}$$

where C is the properly sized observation matrix and v_k is the white measurement noise related with the measuring device used. The additive white-noise vectors w_k and v_k are Gaussian and uncorrelated from each other with zero mean and covariances Q and R, respectively. The state of the system is assumed to be unknown, and therefore, the aim of the estimation process is to find a MMSE estimate of the state $x^{\wedge}_{k|k}$ which is given by

$$\hat{x}_{k|k} \stackrel{\Delta}{=} E\{x_k \mid Y^k\} \tag{3}$$

where $Y^k = ^{\Delta} \{y1 , y 2 ,..., yk \}$ and E{x|y} denotes the expected value of the quantity x ,given the information y . Also, traditionally, one calculates the error estimates given by the covariance matrix $P_{k|k}$ defined as

$$P_{k|k} \stackrel{\Delta}{=} E\{[x_k - \hat{x}_{k|k}][x_k - \hat{x}_{k|k}]^T \mid Y^k\} \tag{4}$$

These direct definitions being too difficult to calculate, recursive forms are adopted for both the state and covariance estimates. The recursive update equations for them are given as

$$\hat{\mathbf{x}}_{k+1|k+1} = \hat{\mathbf{x}}_{k+1|k} + \mathbf{L}_{k+1}\upsilon_{k+1} \quad \text{and}$$

$$\mathbf{P}_{k+1|k+1} = \mathbf{P}_{k+1|k} - \mathbf{L}_{k+1}\mathbf{P}^{\upsilon}_{k+1|k}\mathbf{L}^{\mathrm{T}}_{k+1} \tag{5}$$

where the vectors $x\hat{}_{k+1|k}$ (State Prediction), υ_{k+1} (Innovation) and the matrices L_{k+1} (Kalman Gain), Pk+1|k (State Prediction Covariance), and $P_{k\upsilon+1|k}$ (Innovation Covariance) are dependent on the quantities $x\hat{}_{k|k}$ and $P_{k|k}$ with the following equations.

$$\hat{\mathbf{x}}_{k+1|k} \overset{\Delta}{=} \mathrm{E}\{\mathbf{f}(\mathbf{x}_k, \mathbf{u}_k) \mid \mathbf{Y}^k\} \quad \text{and}$$

$$\mathbf{P}_{k+1|k} \overset{\Delta}{=} \mathrm{E}\{[\mathbf{x}_{k+1} - \hat{\mathbf{x}}_{k+1|k}][\mathbf{x}_{k+1} - \hat{\mathbf{x}}_{k+1|k}]^{\mathrm{T}} \mid \mathbf{Y}^k\} \tag{6}$$

$$\hat{\mathbf{z}}_{k+1|k} = \mathbf{C}\hat{\mathbf{x}}_{k+1|k} \quad \text{and} \quad \upsilon_{k+1} \overset{\Delta}{=} \mathbf{y}_{k+1} - \hat{\mathbf{y}}_{k+1|k} \tag{7}$$

$$\mathbf{P}^{\upsilon}_{k+1|k} = \mathbf{C}\mathbf{P}_{k+1|k}\mathbf{C}^{\mathrm{T}} + \mathbf{R}, \quad \mathbf{K}_{k+1} = \mathbf{P}^{xy}_{k+1|k}(\mathbf{P}^{\upsilon}_{k+1|k})^{-1} \quad \text{and} \quad \mathbf{P}^{xy}_{k+1|k} = \mathbf{P}_{k+1|k}\mathbf{C}^{\mathrm{T}} \tag{8}$$

The quantities $x\hat{}_{k+1|k}$ and $P_{k+1|k}$, which are called state prediction and prediction covariance of the state, respectively. They are vital for the overall filter performance. Eqn.6 do not specify how these quantities are calculated. EKF assumes that errors in the state estimates are small enough to approximate Eqn.6 to their first order Taylor series. As a result, $x\hat{}_{k+1|k}$ and $P_{k+1|k}$ are calculated in EKF as follows;

$$\hat{\mathbf{x}}^{\mathrm{EKF}}_{k+1|k} = \mathbf{f}(\hat{\mathbf{x}}_{k|k}, \mathbf{u}_k) \quad \text{and} \quad \mathbf{P}^{\mathrm{EKF}}_{k+1|k} = \nabla \mathbf{f}_x \mathbf{P}_{k|k} \nabla \mathbf{f}_x{}^{\mathrm{T}} + \mathbf{Q} \tag{9}$$

Where, ∇f_x denotes the Jacobian matrix of the function f with respect to the state x. This linearization in EKF frequently yields wrong results in the estimates of the covariance and thus the state. UKF solves the prediction problem by sampling the distribution of the state in a deterministic manner and then transforming each of the samples using the nonlinear state transition equation. The *n* -dimensional random variable x_k with mean $x\hat{}_{k|k}$ and covariance $P_{k|k}$ is approximated by 2*n* +1 weighted samples or *sigma points* selected by the algorithm.

$$\chi_0(k \mid k) \overset{\Delta}{=} \hat{\mathbf{x}}_{k|k} \quad W_0 \overset{\Delta}{=} \kappa/(n+\kappa) \quad \text{and} \quad \chi_i(k \mid k) \overset{\Delta}{=} \hat{\mathbf{x}}_{k|k} + (\sqrt{(n+\kappa)(\mathbf{P}_{k|k} + \mathbf{Q})})_i \tag{10}$$

$$W_i \triangleq 1/(2(n+\kappa)) \quad , \quad \chi_{i+n}(k|k) \triangleq \hat{x}_{k|k} - (\sqrt{(n+\kappa)(P_{k|k}+Q)})_i$$

$$W_{i+n} \triangleq 1/(2(n+\kappa)) \tag{11}$$

for i = 1,… , n where $\kappa \in \Re$ is a free real number such that $n + \kappa \neq 0$, $((n+\kappa)(P_{k|k} + Q)_i$ is the ith column of the matrix, square root of $(n + \kappa)(Pk|k\ Q)$, and W_i is the weight associated with the ith point. Given these set of samples, the prediction process is as;

(i) Each sigma point is transformed through the process dynamics f ;

$$\chi_i(k+1|k) = f(\chi_i(k|k), u_k) \tag{12}$$

(ii) The state prediction is computed as;

$$\hat{x}_{k+1|k} = \sum_{i=0}^{2n} W_i \chi_i(k+1|k) \tag{13}$$

(iii) The prediction covariance is calculated as;

$$P_{k+1|k} = \sum_{i=0}^{2n} W_i [\chi_i(k+1|k) - \hat{x}_{k+1|k}] \cdot [\chi_i(k+1|k) - \hat{x}_{k+1|k}]^T \tag{14}$$

The equations (13) and (14) replace (6). The other UKF operations are the same as (13) to (14). Note that, operations in the new set of equations composed by (13), (14), (7) and (8) together with measurement updates given in (1) and (2) use only standard vector and matrix operations and need no approximations for both derivative and Jacobian. Also, the order of calculation is the same as that of EKF.

3. SIMULATION RESULTS

A number of simulations were carried out to verify the performance of the state estimation, particularly of the speed estimation with UKF. In Figure 2 – Figure 7, the state estimation performance of UKF is simulated and in Figures 8 and 9 accuracies obtained from EKF and UKF are compared for the speed estimation. Figure 2 shows the actual state variables of the motor; stator currents, rotor fluxes and rotor speed at no-load in a high speed reversal scheme. Figure 3 shows corresponding estimated state variables with UKF under the same conditions. There are almost no differences between the actual and the estimated variables.

Figure 4 and Figure 5 illustrates magnified estimated speed waveforms at no-load in four quadrant high speed and low speed reversal schemes respectively. Both the high speed and low speed estimated waveforms confirm that UKF's performance is quite good in speed estimation for all quadrants without causing instability.

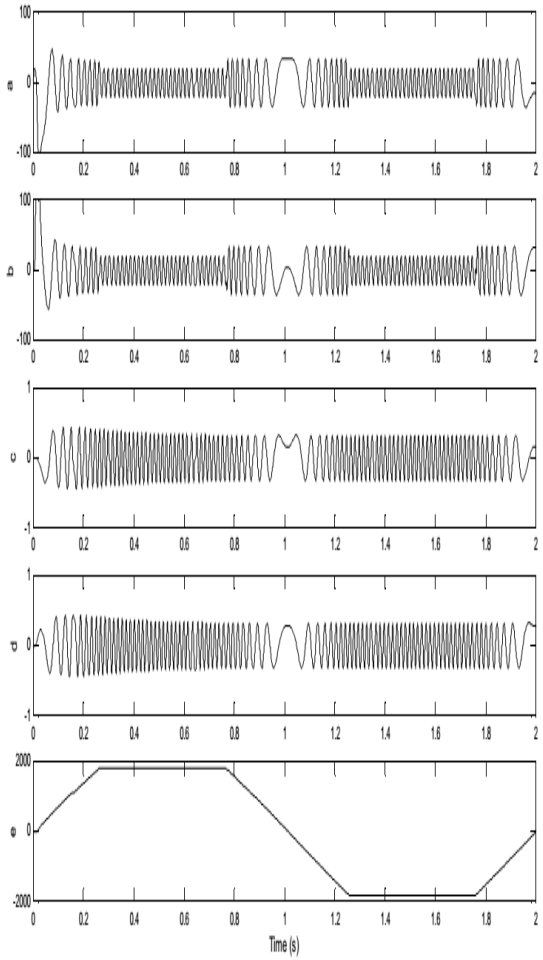

Figure 2 Actual states at no load

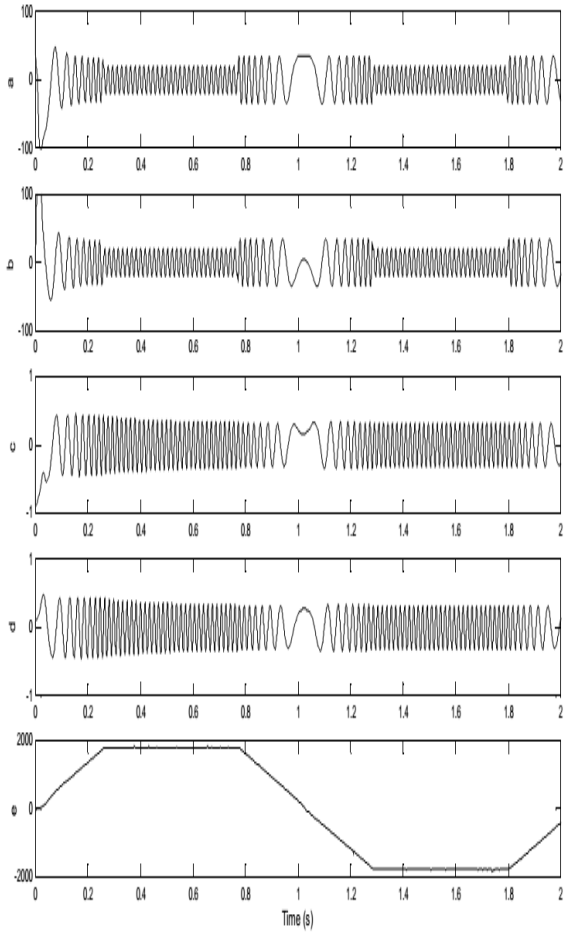

Figure 3 Estimated states with UKF at no load

(a-b) d-q axis stator currents, (c-d) d-q axis rotor fluxes, e) rotor speed (a-b) estimated d-q axis stator currents, (c-d) Estimated. d-q axis rotor fluxes, (e) estimated rotor speed.

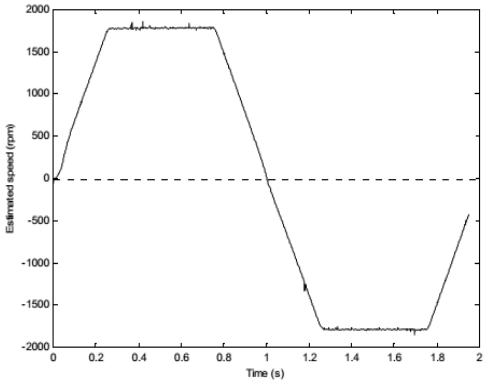

Figure 4 Estimated speed at no-load quadrant high speed reversal (in rpm).rpm)

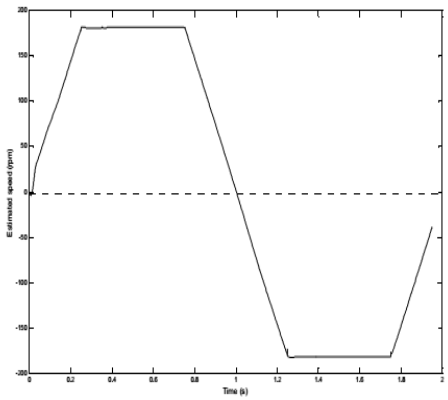

Figure 5 Estimated speed at no-load four quadrant low speed reversal (in rpm)

In Figure 6, estimated state variables of the induction motor are shown under 100 % rated load torque and 100 % rated speed conditions. In addition to high performance at no-load, UKF gives quite satisfactory results under full-load condition. In Figures 7 and 8, actual and estimated speed characteristics are given on top of each other for 100 % and 10 % rated torque and speed case. In the transient part of the waveforms, there appears a difference between the estimated and actual values which is the result of the fact that, in induction motor model, the speed is considered as a constant parameter and corrected only in the measurement updates of the UKF. In simulation tests, we also noticed that there usually exists a small steady-state error between the estimated and actual speed values but that seems to be at negligible levels.

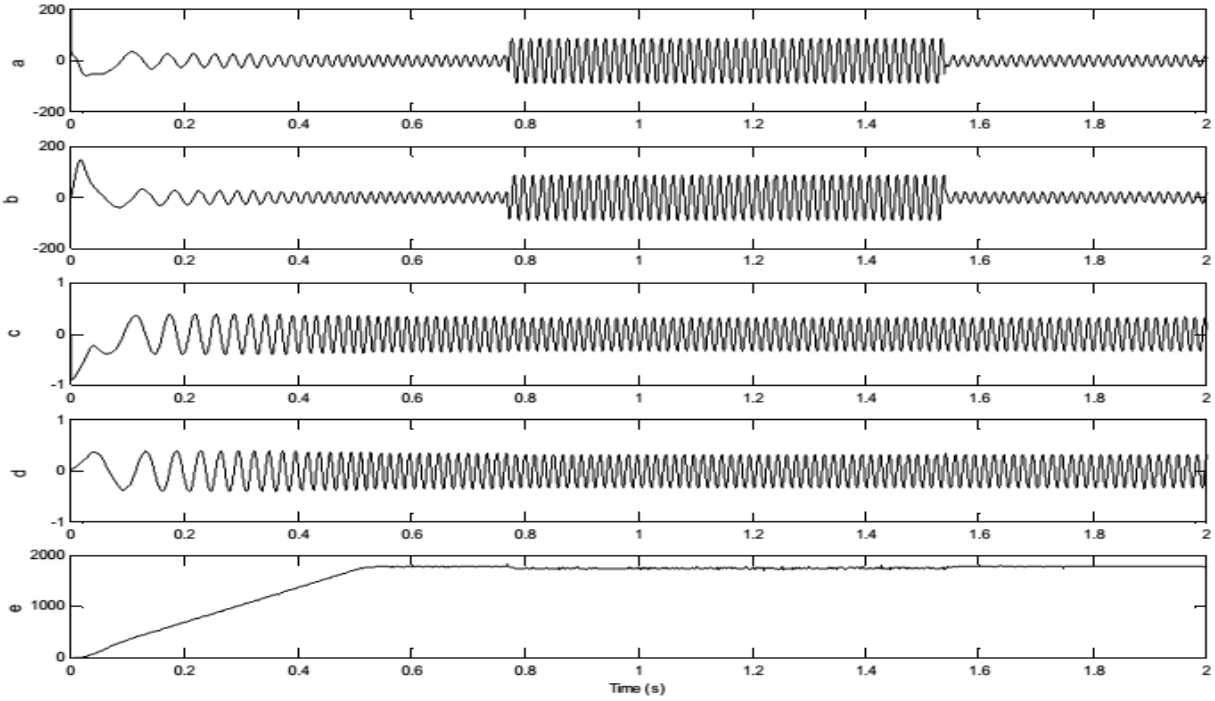

Figure 6 Estimated states at 100 % rated torque and speed (a-b)
(a-b) estimated d-q axis stator currents, (c-d) estimated d-q axis rotor fluxes, (e) estimated rotor speed

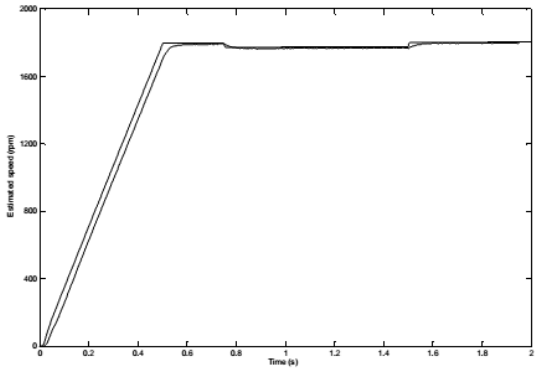

Figure 7 Estimated speed at 100 % rated torque and speed

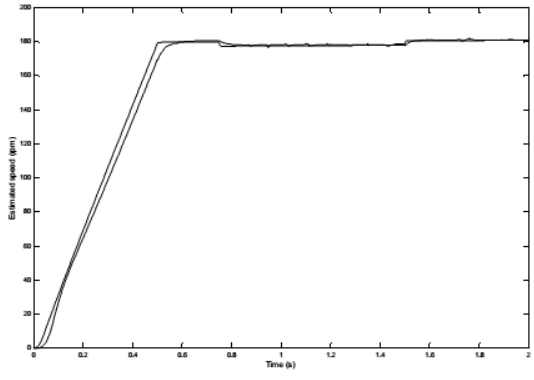

Figure 8 Estimated speed at %10 rated torque and speed

It has been shown that UKF is as good as EKF at least in state observation, and it yields even slightly better speed estimation performance than EKF. This result encourages further study in the area to obtain better state estimation performances for nonlinear systems to overcome the well-known defects of EKF and other traditional nonlinear filtering techniques.

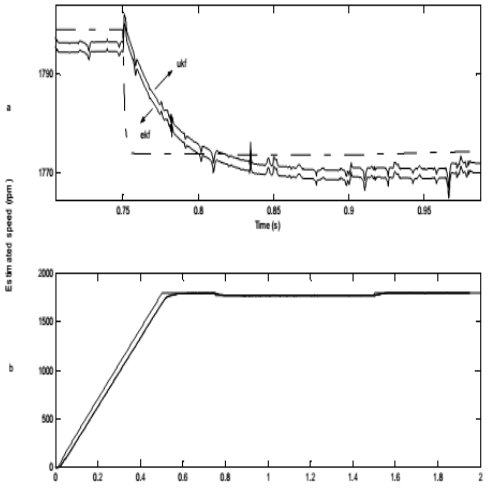

(a) graphics in (b) zoomed at the loading initiation.

Figure 9 Estimated speed optimized for steady state performance at 100 %rated torque and speed using EKF and UKF

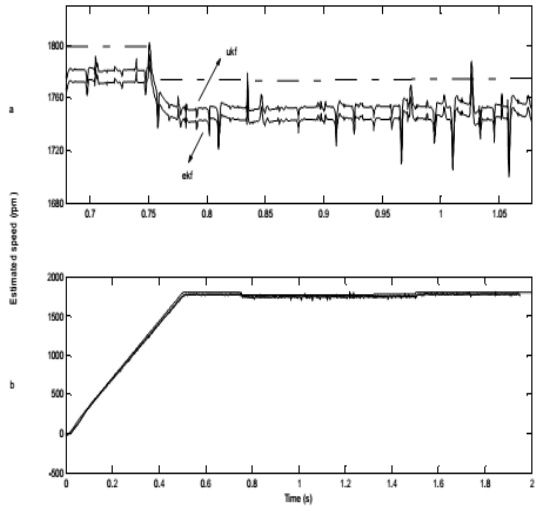

a) graphics in (b) zoomed at the loading initiation

Figure 10 Estimated speed optimized for transient performance at 100 % rated torque and speed using EKF and UKF

4. EXPERIMENTAL SETUP USING DSP PROCESSOR

Among the most important parts of the control and estimation process is the implementation platform. The choice of DSPs is more natural, as many have built-in pulse-width modulation (PWM) channels, analog-to-digital converters (ADCs), and even support speed encoder inputs. A natural companion to any control and estimation platform is an interface board that links this platform to the rest of the system. Such a board is essential when signals into and out of the platform are at power or voltage levels incompatible with the rest of the system. This board can also provide electrical isolation between the platform and high-power components, conditioning of sensor outputs, and amplification of the DSP outputs. Another essential subsystem is the three-phase inverter, which provides the machine with variable-frequency variable-amplitude threephase voltages. The commands and monitoring can be available through a GUI, where the computer communicates with the DSP and the load simultaneously. An elaborate version of Figure 1 is shown in Figure 11 and shows more details. Figure 11 shows several important steps when building an induction machine drive for testing the control and estimation. These steps are summarized in Figure 12, where the GUI is built in MATLAB/Simulink, and

the DSP is programmed in Code Composer Studio (CCS). Simulink provides a user-friendly control and estimation interface where the designer can use signal-flow block diagrams similar to a simulation. The block diagrams built can then be automatically translated to C-code that can be compiled in CCS. It is essential that discrete-time blocks with fixed sampling rates and fixed point math be used in the block diagram, although floating-point DSPs are currently available. The testing and calibration are first done with no load, then under different loads for further tuning and calibration. Appropriate scaling and filtering of all measured signals is essential, and even though the interface stage could help reduce noise and manage offsets, more digital filtering and scaling is required. The work presented here employs an eZdsp F2812™ board as the control and estimation platform. This board is built around the TMS320F2812 DSP.

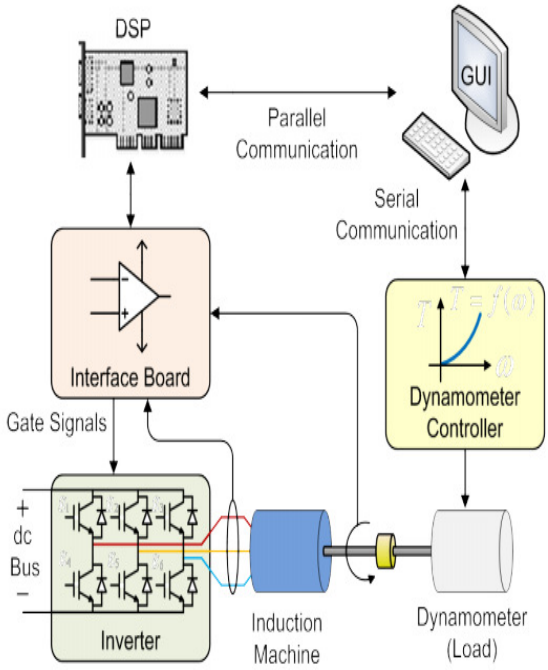

Figure 11 Detailed laboratory setup

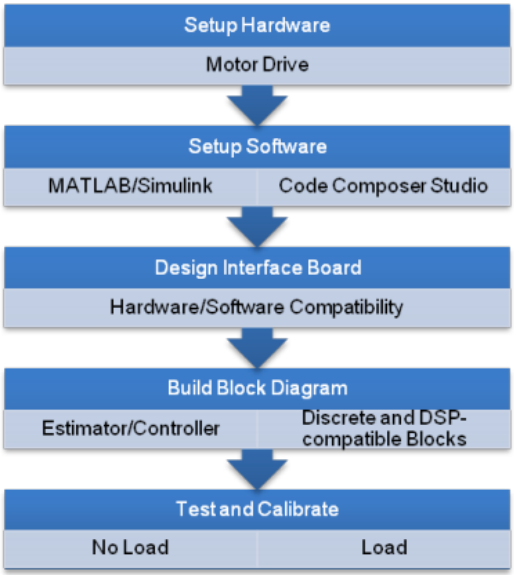

Figure 12 Implementation procedure of the control and estimation

This platform is compatible with Simulink®, and includes six dual pulse PWM channels (12 channels total), 16 ADCs, and a speed encoder input. The processor is a 32-bit DSP with fixed-point arithmetic; thus, discrete and fixed-point math blocks of Simulink can be used in the block diagrams. Once programmed, the DSP can run independent from Simulink, but the link is maintained through parallel communication for an interactive GUI. The GUI allows to place speed and flux commands, and monitor estimates in real time. For this platform, two primary software packages are available on the host computer where the development and control take place: MATLAB/Simulink, which support math and control development, and CCS, which supports detailed code development for the DSP. MATLAB is used to build the GUI for real-time communication with the DSP using real-time data exchange (RTDX) channels. These channels are set in the block diagram. PWM channels send gate signals to the switches in the three-phase inverter, and can be used as access points to monitor signals on an oscilloscope or logic

analyzer. On the hardware side, current and voltage sensors are built in the inverter. The interface board is used to amplify signals sent from the DSP to the inverter, and to filter and scale signals sent from the sensors to the DSP. , the eZdspF2812 requires all ADC inputs to be between 0 and 3 V. While simple voltage dividers with limited currents are straightforward, many current sensors have dc offsets and nonlinear input/output relations. After the sensors are scaled and conditioned for the ADC, we can read sensor and estimation information in Simulink.

5. EXPERIMENTAL RESULTS AND CONCLUSION

While obtaining the experimental results, the real time stator voltages and currents are processed in Matlab with the associated EKF and UKF programs. Figure 13 shows estimations of states I&II (dq axis stator currents) made by EKF and the actual states I&II measured from the experimental setup. It may easily be noticed that the estimated states are quite close to the measured ones. Figure 14 shows the estimated dq axis rotor fluxes in stationary reference frame. The magnitude of the rotor flux justifies that the estimated dq components of the rotor flux do not involve dc offset and orthogonal to each other. In order to examine the rotor speed (state V) estimation performance of EKF experimentally under varying speed conditions, a trapezoidal speed reference command is embedded into the DSP code.

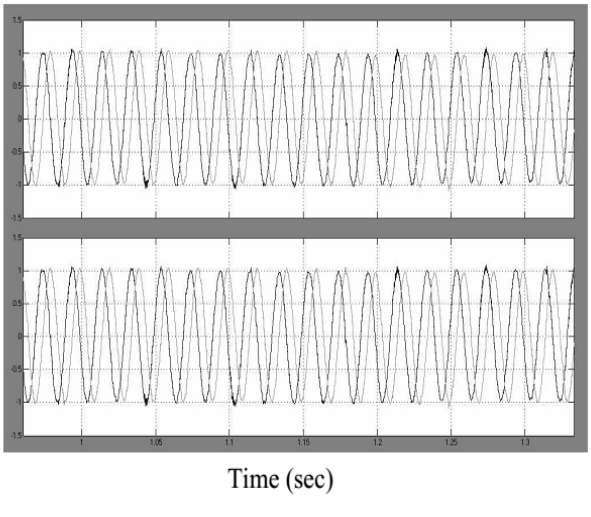

Figure 13 The estimated & measured states I and II by EKF III by EKF and the flux

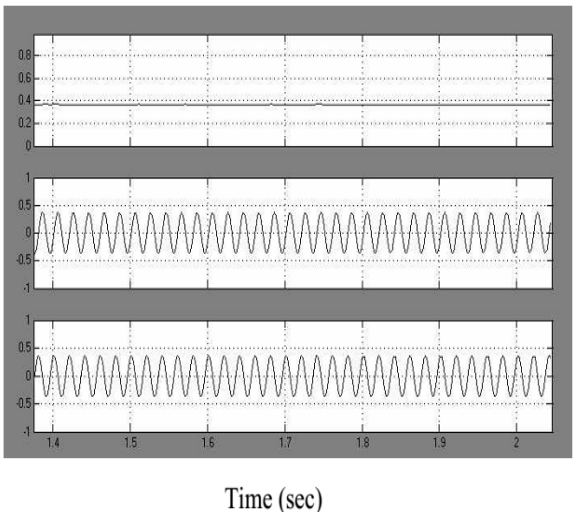

Figure 14 The estimated states II and magnitude of the rotor flux

As shown in Figure 15, EKF rotor speed estimation successfully tracks the trapezoidal path The same states of the induction motor model estimated by EKF are also estimated by UKF. Figure 16 shows estimations of states I&II (dq axis stator currents) made by UKF and the actual states I&II measured from the experimental setup.

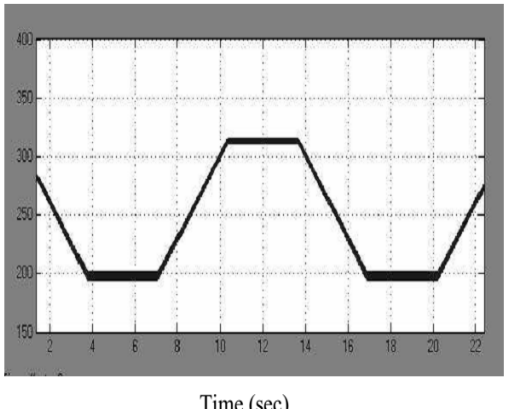

Figure 15 Rotor speed tracking performance of EKF obtained by EKF states I and II (lower one)

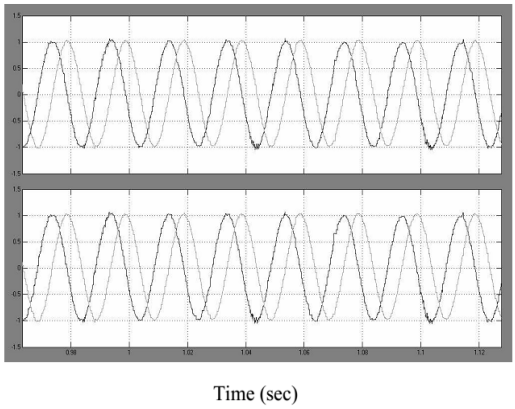

Figure 16 The estimated and measured states I and II

One may easily notice that the estimated states are quite close to the measured ones. Figure 17 shows the estimated dq axis rotor fluxes in stationary reference frame by UKF. The magnitude of the rotor flux justifies that the estimated dq components of the rotor flux are estimated accurately In order to compare both types of the observers, EKF and UKF, the covariance matrices regarding to both types have been initialized with the same entries under the same operating conditions. The estimated rotor speed waveforms, when plotted together as shown in Figure 18, confirm that the estimation accuracy of UKF is superior over EKF as claimed before when discussing the simulation results related to both observer design techniques

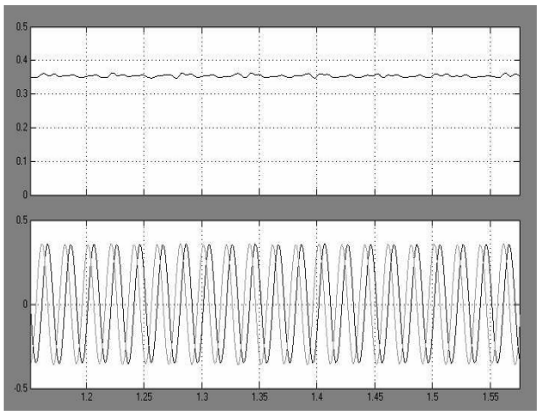

Figure 17 The estimated states II and III by UKF and EKF (lighter) and the magnitude of the rotor flux

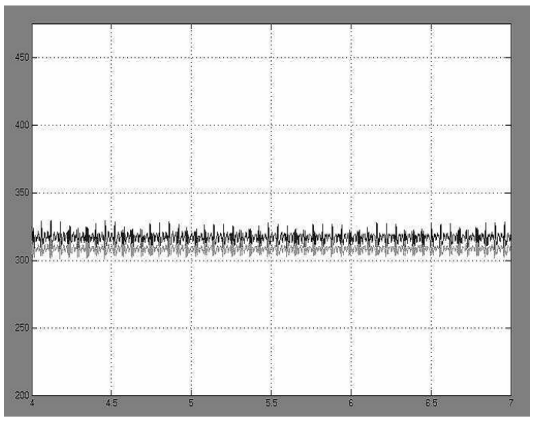

Figure 18 Rotor speed waveforms by UKF (darker) under the same experimental conditions

The simulation results were shown in Figure 9 and Figure 10 As expected from simulations, the speed estimation accuracy of UKF is better than EKF under the same experimental conditions. The measured speed from the motor shaft is 314 rad/sec. The mean of the state estimation error in UKF is 2.65 rad/sec at steady state, and that in EKF is 5.8 rad/sec. This result shows that the estimates of EKF have serious bias problems compared to UKF. As discussed earlier, the derivative free algorithm of

UKF without a linearity approximation contributes its estimates positively. Furthermore, the noise sampling feature of UKF is more realistic approach instead of assuming the noise directly as Gaussian. This property also makes its estimation accuracy better than EKF.

REFERENCES

[1] Atkinson, D., Acarnley, P. and Finch, J. W. Observers for Induction Motor State and Parameter Est. *IEEE Tran. IA,* **27**(6), Dec. 1991, pp. 1119–1127.

[2] Julier and Uhlmann, J. K. A new extension of the Kalman filter to non linear systems. Available: http://www.robots.ox.ac.uk.

[3] Julier, S., Uhlmann, J. K. and Durrant-Whyte, H. F. A new method for the nonlinear transformation of means and covariances in filters and estimators. *IEEE Trans. Automatic Control*, **45**, March 2000, pp. 477–482.

[4] Julier, S., Uhlmann, J. K. and Durrant-Whyte, H. F. A new approach for filtering nonlinear systems. Available: http://www.robots.ox.ac.uk

[5] Kim, H. W. and Sul, S. K. A New Motor Speed Estimator using Kalman Filter in Low Speed Range. *IEEE Tran. IE,* **43**(4), Aug.1996, pp. 498–504.

[6] Kim, R., Sul, S. K. and Park, M. H. Speed Sensorless Vector Control of Induction Motor Using Extended Kalman Filter. *IEEE Tran. IA*, 30(5), Oct. 1994, pp. 1225–1233.

[7] Zai, L. C., De Marco, C. L. and Lipo, T. A. An Extended Kalman Filter Approach to Rotor Time Constant Measurement in PWM Induction Motor Drives. *IEEE Tran. IA*, **28**(1), Jan/Feb 1992, pp. 96–104.